

Inverse Seesaw from dynamical $B - L$ breaking

Julia Gehrlein

*Departamento de Física Teórica, Universidad Autónoma de Madrid,
Cantoblanco E-28049 Madrid, Spain
Instituto de Física Teórica UAM/CSIC,
Calle Nicolás Cabrera 13-15, Cantoblanco E-28049 Madrid, Spain*

The Inverse Seesaw scenario relates the smallness of the neutrino masses to a small $B - L$ breaking parameter. We investigate a possible dynamical generation of the Inverse Seesaw neutrino mass mechanism from the spontaneous breaking of a gauged $U(1)_{B-L}$. To obtain an anomaly free theory we need to introduce additional fermions which exhibit an interesting phenomenology. Additionally, we predict a Z' boson associated to the broken $B - L$ which preferentially interacts with the dark sector formed by the extra fermions making it particularly *elusive*.

1 Introduction

The observation of non-zero neutrino masses is so far the only laboratory-based evidence for physics beyond the Standard Model. Nevertheless, there are many ways to generate neutrino masses. The probably simplest way is via the Seesaw framework^{1,2,3,4,5,6} where the smallness of the neutrino masses is explained with a large suppression of the electroweak scale. However, this is not the only possibility to explain the smallness of neutrino masses. The inverse seesaw (ISS)⁷ relies on the fact that neutrino masses are protected by the $B - L$ global symmetry. If this symmetry is only mildly broken, neutrino masses will be suppressed by this small $B - L$ -breaking parameters. On the other hand, production and detection of the extra ISS right-handed neutrinos at colliders as well as their indirect effects in flavour and precision electroweak observables are not protected by this symmetry hence leading to a rich and interesting phenomenology.

To explore a possible dynamical origin of the ISS pattern we choose to gauge $B - L$ which then gets spontaneously broken⁸.

2 The model

In the ISS the masses of the light neutrinos are given by

$$m_\nu \sim v^2 Y_\nu M_N^{-1} \mu (M_N^T)^{-1} Y_\nu^T. \quad (1)$$

With TeV-scale right handed neutrinos and $\mathcal{O}(1)$ Yukawa couplings $\mu \sim \mathcal{O}(\text{keV})$. Since a hierarchy of mass scales $\mu/v_H \sim 10^{-6}$ seems to be rather ad hoc we will promote μ to a dynamical quantity by gauging $B - L$ and identify the μ parameter with the $B - L$ breaking scalar vev.

For the ISS two copies of right-handed neutrinos (N_R , N'_R) with $B - L$ charges $+1$ and -1 per active neutrino are introduced.

Requiring an anomaly-free theory leads to the introduction of additional chiral fermion content to the model. We find a phenomenologically interesting and viable scenario for the

Table 1: Neutral fermions and singlet scalars with their $U(1)_{B-L}$ charge and their multiplicity. $\phi_{1,2}$ are SM singlet scalars while N_R , N'_R and χ_R are right-handed and χ_L and ω are left-handed SM singlet fermions respectively.

Particle	ϕ_1	ϕ_2	ν_L	N_R	N'_R	χ_R	χ_L	ω
$U(1)_{B-L}$ charge	+1	+2	-1	-1	+1	+5	+4	+4
Multiplicity	1	1	3	3	3	1	1	1

particle content displayed in tab. 1. The Lagrangian in the neutrino sector is then given by

$$-\mathcal{L}_\nu = \bar{L}Y_\nu\tilde{H}N_R + \overline{N_R^c}M_NN'_R + \phi_2\overline{N_R^c}Y_NN_R + \phi_2^*\overline{(N'_R)^c}Y'_NN'_R + \phi_1^*\overline{\chi_L}Y_\chi\chi_R + \text{h.c.} \quad (2)$$

The scalar potential of the model can be written as

$$V = \frac{m_H^2}{2}H^\dagger H + \frac{\lambda_H}{2}(H^\dagger H)^2 + \frac{m_1^2}{2}\phi_1^*\phi_1 + \frac{m_2^2}{2}\phi_2^*\phi_2 + \frac{\lambda_1}{2}(\phi_1^*\phi_1)^2 + \frac{\lambda_2}{2}(\phi_2^*\phi_2)^2 \\ + \frac{\lambda_{12}}{2}(\phi_1^*\phi_1)(\phi_2^*\phi_2) + \frac{\lambda_{1H}}{2}(\phi_1^*\phi_1)(H^\dagger H) + \frac{\lambda_{2H}}{2}(\phi_2^*\phi_2)(H^\dagger H) - \eta(\phi_1^2\phi_2^* + \phi_1^{*2}\phi_2). \quad (3)$$

Minimalisation of the potential yields a vev for ϕ_2

$$v_2 \simeq \frac{\sqrt{2}\eta v_1^2}{m_2^2}, \quad (4)$$

which will be identified with the μ parameter. To obtain $v_2 \sim \mathcal{O}(\text{keV})$, one could have $m_2 \sim 10 \text{ TeV}$, $v_1 \sim 10 \text{ TeV}$, and $\eta \sim 10^{-5} \text{ GeV}$.

With the conventions $\phi_j = (v_j + \varphi_j + i a_j)/\sqrt{2}$ the mixing angles α_1 and α_2 between $h - \varphi_1$ and $\varphi_1 - \varphi_2$, respectively, are given by

$$\tan \alpha_1 \simeq \frac{\lambda_{1H}}{\lambda_1} \frac{v}{2v_1}, \quad \text{and} \quad \tan \alpha_2 \simeq 2 \frac{v_2}{v_1}. \quad (5)$$

With $v_1 \sim \text{TeV}$ and the quartics λ_1 and λ_{1H} are $\mathcal{O}(1)$, the mixing α_1 is expected to be small but non-negligible. Due to this mixing the couplings of the Higgs to gauge bosons and fermions get diminished. Relative to the SM couplings they are

$$\kappa_F = \kappa_V = \cos \alpha_1, \quad (6)$$

which is constrained to be $\cos \alpha_1 > 0.92$ (or equivalently $\sin \alpha_1 < 0.39$)⁹.

The Z' gauge boson associated to the broken $B - L$ obtains a mass

$$M_{Z'} = g_{\text{BL}} \sqrt{v_1^2 + 4v_2^2} \simeq g_{\text{BL}} v_1. \quad (7)$$

As the largest particles with the largest $B - L$ charges are in the dark sector of the model (the massless Weyl fermion ω and χ_R , χ_L which will form a Dirac pair), the Z' is very elusive and has a large BR of 70% to invisibles.

The Dirac fermion χ is stable since it is protected by an accidental $U(1)$ symmetry in the dark sector, hence it is a good DM candidate. Its main annihilation channels are $\chi\bar{\chi} \rightarrow f\bar{f}$ via the Z' boson exchange and $\chi\bar{\chi} \rightarrow Z'Z'$ - if kinematically allowed.

The DM Z' interaction leads to a spin-independent scattering in direct detection experiments. With the current experimental bound on the spin-independent cross section we can derive a lower bound on the vev of ϕ_1 :

$$v_1 [\text{GeV}] > \left(\frac{2.2 \cdot 10^9}{\sigma_\chi^{\text{DD}} [\text{pb}]} \right)^{1/4}. \quad (8)$$

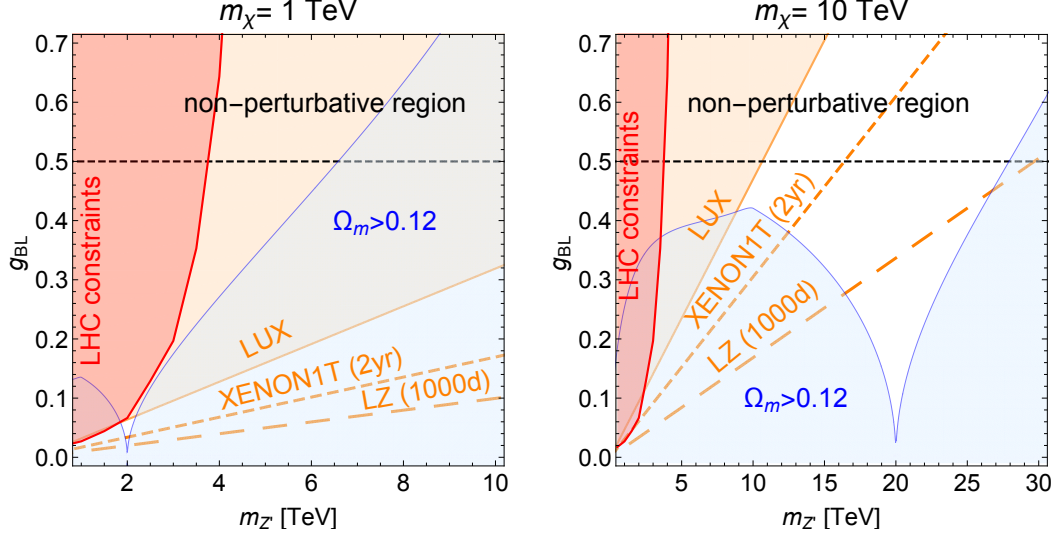


Figure 1 – Summary plots of our results for DM masses of $m_\chi = 1$ TeV and 10 TeV. The red region to the left is excluded by LHC constraints on the Z' , the region above $g_{BL} > 0.5$ is non-perturbative due to $g_{BL} \cdot q_{\max} \leq \sqrt{2\pi}$. In the blue shaded region DM is overabundant. The orange coloured region is already excluded by direct detection constraints from LUX, the short-dashed line indicates the future constraints from XENON1T (projected sensitivity assuming $2t \cdot y$), the long-dashed line the future constraints from LZ (projected sensitivity for 1000d of data taking).

This bound pushes the DM mass to be $m_\chi \gtrsim \text{TeV}$. For example, for $g_{BL} = 0.25$ and $m_{Z'} = 10$ TeV, a DM mass $m_\chi = 3.8$ TeV is needed to have $\sigma_\chi^{\text{DD}} \sim 9 \times 10^{-10}$ pb. In turn, this bound translates into a lower limit on the vev of ϕ_1 : $v_1 \gtrsim 40$ TeV (with $Y_\chi \gtrsim 0.1$).

Since the main annihilation channel of χ is via the Z' which couples dominantly to the dark sector, the bounds from indirect detection searches turn out to be subdominant.

The massless fermion ω contributes to the relativistic degrees of freedom in the early universe. Comparing the Hubble expansion rate of the Universe with the interaction rate leads to a freeze out temperature of ω (for values that satisfy the correct DM relic abundance) of $T_\omega^{\text{f.o.}} \sim 4$ GeV, before the QCD phase transition.

This means that the SM bath will heat significantly after ω decouples which suppresses the contribution of ω to the number of degrees of freedom in radiation:

$$\Delta N_{\text{eff}} \approx 0.026 \quad (9)$$

which is one order of magnitude smaller than the current uncertainty on $N_{\text{eff}}^{\text{exp}} = 3.04 \pm 0.33$ ¹⁰. Nevertheless, this deviation from N_{eff} could be detected by EUCLID-like survey^{11,12} and would be an interesting probe of the model in the future.

More details on the model can be found in⁸.

3 Summary of the results

Our results are summarised in fig. 1 for different DM masses of $m_\chi = 1$ TeV and 10 TeV.

The red region to the left is constrained by recasted LHC $Z' \rightarrow e^+e^-, \mu^+\mu^-$ resonant searches^{13,14}.

In the blue region the relic abundance is too large and the orange region displays the excluded regions from current direct detection experiments¹⁵, the dashed lines show the sensitivity of near future experiments (XENON1T¹⁶ (projected sensitivity assuming $2t \cdot y$), the long-dashed line the future constraints from LZ¹⁷ (projected sensitivity for 1000d of data taking)). For gauge couplings above the grey dashed line perturbativity will be lost ($g_{BL} \cdot q_{\max} \leq \sqrt{2\pi}$ with largest $B - L$ charge $q_{\max} = 5$).

In summary, we have presented a dynamical realisation of the inverse seesaw scenario which predicts a DM candidate at the TeV scale which can lead to the correct relic abundance while evading all current direct and indirect detection constraints, a massless fermion which contributes to N_{eff} , an elusive Z' at the TeV scale and two scalars with masses around 10 TeV. Additionally, our model exhibits the phenomenology of the right-handed neutrinos of the usual inverse seesaw.

Acknowledgments

JG is supported by the EU grants H2020-MSCA-ITN-2015/674896-Elusives. JG thanks the organisers of Moriond 2018 EW for the financial support that allowed her to attend the conference.

References

1. Peter Minkowski. $\mu \rightarrow e\gamma$ at a Rate of One Out of 10^9 Muon Decays? *Phys. Lett.*, B67:421–428, 1977.
2. Pierre Ramond. The Family Group in Grand Unified Theories. In *International Symposium on Fundamentals of Quantum Theory and Quantum Field Theory Palm Coast, Florida, February 25-March 2, 1979*, pages 265–280, 1979.
3. Murray Gell-Mann, Pierre Ramond, and Richard Slansky. Complex Spinors and Unified Theories. *Conf. Proc.*, C790927:315–321, 1979.
4. Tsutomu Yanagida. HORIZONTAL SYMMETRY AND MASSES OF NEUTRINOS. *Conf. Proc.*, C7902131:95–99, 1979.
5. Rabindra N. Mohapatra and Goran Senjanovic. Neutrino Mass and Spontaneous Parity Violation. *Phys. Rev. Lett.*, 44:912, 1980.
6. J. Schechter and J. W. F. Valle. Neutrino Masses in $SU(2) \times U(1)$ Theories. *Phys. Rev.*, D22:2227, 1980.
7. R. N. Mohapatra and J. W. F. Valle. Neutrino Mass and Baryon Number Nonconservation in Superstring Models. *Phys. Rev.*, D34:1642, 1986.
8. Valentina De Romeri, Enrique Fernandez-Martinez, Julia Gehrlein, Pedro A. N. Machado, and Viviana Niro. Dark Matter and the elusive Z' in a dynamical Inverse Seesaw scenario. *JHEP*, 10:169, 2017.
9. Georges Aad et al. Measurements of the Higgs boson production and decay rates and constraints on its couplings from a combined ATLAS and CMS analysis of the LHC pp collision data at $\sqrt{s} = 7$ and 8 TeV. *JHEP*, 08:045, 2016.
10. P. A. R. Ade et al. Planck 2015 results. XIII. Cosmological parameters. *Astron. Astrophys.*, 594:A13, 2016.
11. Tobias Basse, Ole Eggers Bjaelde, Jan Hamann, Steen Hannestad, and Yvonne Y. Y. Wong. Dark energy properties from large future galaxy surveys. *JCAP*, 1405:021, 2014.
12. Luca Amendola et al. Cosmology and Fundamental Physics with the Euclid Satellite. 2016.
13. Vardan Khachatryan et al. Search for narrow resonances in dilepton mass spectra in proton-proton collisions at $\sqrt{s} = 13$ TeV and combination with 8 TeV data. *Phys. Lett.*, B768:57–80, 2017.
14. The ATLAS collaboration. Search for new high-mass resonances in the dilepton final state using proton-proton collisions at $\sqrt{s} = 13$ TeV with the ATLAS detector. 2016.
15. D. S. Akerib et al. Results from a search for dark matter in the complete LUX exposure. *Phys. Rev. Lett.*, 118(2):021303, 2017.
16. E. Aprile et al. Physics reach of the XENON1T dark matter experiment. *JCAP*, 1604(04):027, 2016.
17. D. S. Akerib et al. LUX-ZEPLIN (LZ) Conceptual Design Report. 2015.